J. Fluid Mech. (2008), *vol.* 605, *pp.* 263–279.
doi:10.1017/S0022112008001523 Printed in the United Kingdom

Transient inertial hydrodynamic interaction between two identical spheres settling at small Reynolds number

B. U. FELDERHOF

Institut für Theoretische Physik A, RWTH Aachen, Templergraben 55, 52056 Aachen, Germany
ufelder@physik.rwth-aachen.de

(Received 7 November 2007 and in revised form 10 March 2008)

The flow pattern generated by a sphere accelerated from rest by a small constant applied force shows scaling behaviour at long times, as can be shown from the solution of the linearized Navier–Stokes equations. In the scaling regime the kinetic energy of the flow grows with the square root of time. For two distant settling spheres starting from rest the kinetic energy of the flow depends on the distance vector between centres; owing to interference of the flow patterns. It is argued that this leads to relative motion of the two spheres. The corresponding interaction energy is calculated explicitly in the scaling regime.

1. Introduction

When a sphere immersed in a quiescent viscous incompressible fluid is accelerated from rest by a constant applied force, starting at time $t = 0$, it starts to move with initial acceleration corresponding to the sum of its own mass and the added mass of the surrounding fluid. The added mass can be calculated from the theory of irrotational flow (Lighthill 1986). If the force is sufficiently small, corresponding to low Reynolds number, the flow pattern and the motion of the sphere at later times can be calculated from the linearized Navier–Stokes equations (Felderhof 2007*a*). The sphere speeds up gradually with decreasing acceleration, and reaches a constant Stokes velocity. The final velocity is used to define the steady-state friction coefficient.

When a pair of identical spheres with initial centre-to-centre vector $\boldsymbol{R}$ is accelerated similarly, then at low Reynolds number they move in tandem at constant $\boldsymbol{R}$ with a time-dependent velocity depending on the distance vector. The distance-dependence is caused by hydrodynamic interactions. Owing to a reciprocity theorem the time-dependent six-dimensional mobility matrix has the same symmetry as for steady-state Stokes flow (Kim & Karrila 1991). It was found experimentally by Jayaweera, Mason & Slack (1964) that two spheres settling side-by-side slowly increase their distance apart. This was ascribed to residual inertial effects (Hocking 1964). In the following we propose a theory for the effect for the limiting case where the initial separation distance is large compared with the sphere radius.

The theory is based on a calculation of the kinetic energy of the flow generated by the two spheres. For a single sphere the kinetic energy grows with time, eventually in proportion to the square root of time, with a coefficient which is universal, i.e. independent of the radius of the sphere, its mass, or the boundary condition applied at the surface. In the long-time limit the flow pattern and the deviation of the sphere velocity from its final Stokes value show universal scaling behaviour. For a pair of

spheres which are sufficiently far apart the generated flow is a linear superposition of two such scaling flow patterns. Since the kinetic energy is quadratic in the local flow velocity there is an interference of flow patterns, and the total kinetic energy depends on the distance vector between centres. We appeal to irreversible thermodynamics (Einstein 1906; Onsager 1931) to argue that this causes an interaction force between the two spheres. We find that in the long-time limit the force is repulsive if the applied force is directed along $\boldsymbol{R}$, but is attractive at large distance if the applied force is transverse to $\boldsymbol{R}$. In the latter case the force becomes repulsive at shorter distance. The distance corresponding to the minimum of kinetic energy, where the interaction force vanishes, grows as the square root of time.

The scaling flow pattern of a single sphere can be found from the Green function of the linearized Navier–Stokes equations. We first discuss the Green function, corresponding to a point particle set in motion by a delta-function force pulse, and show that the kinetic energy of the flow pattern decays with a $t^{-3/2}$ power law. The kinetic energy is calculated conveniently from the Stokes stream function representation of the Green function. We compare this with the kinetic energy of the flow generated by a sphere subject to a force pulse, and show that at long times the latter shows scaling behaviour. Subsequently we perform the same comparison for a sphere subject to a constant force starting at $t = 0$. In this case the energy of the scaling flow pattern increases as $\sqrt{t}$. Finally we consider a pair of identical spheres and calculate the kinetic energy of the total flow in the scaling limit. In this limit we find an explicit expression for the anisotropic interaction energy.

2. Scaling limit

We consider a sphere of radius a and mass m_p immersed in a viscous incompressible fluid of shear viscosity η and mass density ρ. Mixed slip–stick boundary conditions are applied at the surface of the sphere. Elsewhere (Felderhof 2007*b*) we have found the flow pattern after a sudden small impulse applied at the centre of the sphere, as calculated from the linearized Navier–Stokes equations. In the long-time limit the solution shows scaling behaviour, as shown earlier (Cichocki & Felderhof 2000) from a study of the low-frequency limit of the Fourier transform of the flow pattern with respect to time. The scaling behaviour corresponds to the Green function of the linearized Navier–Stokes equations. We first study the Green function in some more detail.

The Green function of the linearized Navier–Stokes equations for a viscous incompressible fluid is a tensor giving the flow velocity at any point in space at any time due to a delta-function force pulse. The fluid is of infinite extent and assumed to be at rest for $t < 0$. We take the force pulse to be applied at the origin at $t = 0$. Then the equations to be solved are

$$\rho\frac{\partial \boldsymbol{v}}{\partial t} = \eta\nabla^2\boldsymbol{v} - \nabla p + \boldsymbol{S}\delta(\boldsymbol{r})\delta(t), \qquad \nabla\cdot\boldsymbol{v} = 0, \tag{1}$$

where $\boldsymbol{v}(\boldsymbol{r}, t)$ is the flow velocity, and $p(\boldsymbol{r}, t)$ is the pressure. Here $\boldsymbol{S}$ has the dimension of momentum. We write the flow velocity for $t > 0$ as

$$\boldsymbol{v}(\boldsymbol{r}, t) = \frac{1}{4\pi\eta}\boldsymbol{T}(\boldsymbol{r}, t)\cdot\boldsymbol{S}. \tag{2}$$

The explicit expression for the tensor $\boldsymbol{T}(\boldsymbol{r}, t)$ was first derived by Oseen (1927). It can also be derived from the Fourier transform of equations (1) with respect to time (Cichocki & Felderhof 2000). The tensor is given by

$$\boldsymbol{T}(\boldsymbol{r}, t) = \mathbf{1}\frac{1}{\sqrt{4\pi\nu}t^{3/2}}\exp(-r^2/4\nu t) + \nu\nabla\nabla\frac{\mathrm{erf}(r/\sqrt{4\nu t})}{r}, \tag{3}$$

where $\nu = \eta/\rho$ is the kinematic viscosity. More explicitly

$$\boldsymbol{T}(\boldsymbol{r}, t) = \frac{\exp(-r^2/4\nu t)}{\sqrt{4\pi\nu t}^{3/2}}\left[\left(1+2\frac{\nu t}{r^2}\right)\mathbf{1}-\left(1+6\frac{\nu t}{r^2}\right)\hat{\boldsymbol{r}}\hat{\boldsymbol{r}}\right]+\nu\frac{-\mathbf{1}+3\hat{\boldsymbol{r}}\hat{\boldsymbol{r}}}{r^3}\mathrm{erf}\left(\frac{r}{\sqrt{4\nu t}}\right). \tag{4}$$

The time-integral of the tensor is

$$\boldsymbol{T}_0(\boldsymbol{r}) = \int_0^\infty \boldsymbol{T}(\boldsymbol{r}, t)\,\mathrm{d}t = \frac{\mathbf{1}+\hat{\boldsymbol{r}}\hat{\boldsymbol{r}}}{2r}. \tag{5}$$

This is the familiar Oseen-tensor solution of the steady-state Stokes equations. The pressure generated by the impulse is

$$p(\boldsymbol{r}, t) = \frac{1}{4\pi}\frac{\hat{\boldsymbol{r}}\cdot\boldsymbol{S}}{r^2}\delta(t). \tag{6}$$

The long-range pressure field is established instantaneously, because the fluid is incompressible. There is a corresponding long-range dipolar flow field, as is evident from the limit $t \to 0+$ in (4),

$$\boldsymbol{T}(\boldsymbol{r}, 0+) = 4\pi\nu\mathbf{1}\delta(\boldsymbol{r}) + \nu\frac{-\mathbf{1}+3\hat{\boldsymbol{r}}\hat{\boldsymbol{r}}}{r^3}. \tag{7}$$

The dipolar flow field decays at later times due to viscous dissipation.

The tensor $\boldsymbol{T}(\boldsymbol{r}, t)$ can be expressed in terms of a Stokes stream function $\Psi_s(\boldsymbol{r}, t)$, since the flow field $\boldsymbol{v}(\boldsymbol{r}, t)$ given by (2) is axisymmetric. The subscript s refers to the scaling limit. Taking the z-axis in the direction of the initial impulse, and introducing polar coordinates (r, θ, φ) in the familiar way (Happel & Brenner 1973) we can write the velocity field as

$$\boldsymbol{v}_s(\boldsymbol{r}, t) = \nabla \times \left(\frac{\Psi_s(r, \theta, t)}{r\sin\theta}\boldsymbol{e}_\varphi\right), \tag{8}$$

with spherical components

$$v_{sr} = \frac{1}{r^2\sin\theta}\frac{\partial\Psi_s}{\partial\theta}, \qquad v_{s\theta} = -\frac{1}{r\sin\theta}\frac{\partial\Psi_s}{\partial r}, \qquad v_{s\varphi} = 0. \tag{9}$$

It follows from (8) that

$$(\boldsymbol{v}_s\cdot\nabla)\Psi_s = 0, \tag{10}$$

so that the stream function is constant along the streamlines. By comparison with (4) the explicit expression is

$$\Psi_s(r, \theta, t) = \frac{S}{4\pi\eta}\chi_s(r, t)\sin^2\theta \tag{11}$$

with radial function

$$\chi_s(r, t) = \frac{\nu}{r}\mathrm{erf}\left(\frac{r}{\sqrt{4\nu t}}\right) - \sqrt{\frac{\nu}{\pi t}}\exp\left(-\frac{r^2}{4\nu t}\right). \tag{12}$$

The stream function is found to satisfy the partial differential equation

$$\frac{\partial\Psi_s}{\partial t} = \nu\mathrm{E}^2\Psi_s, \tag{13}$$

where E^2 denotes the differential operator

$$\mathrm{E}^2 = \frac{\partial^2}{\partial r^2} + \frac{\sin\theta}{r^2}\frac{\partial}{\partial\theta}\left(\frac{1}{\sin\theta}\frac{\partial}{\partial\theta}\right). \tag{14}$$

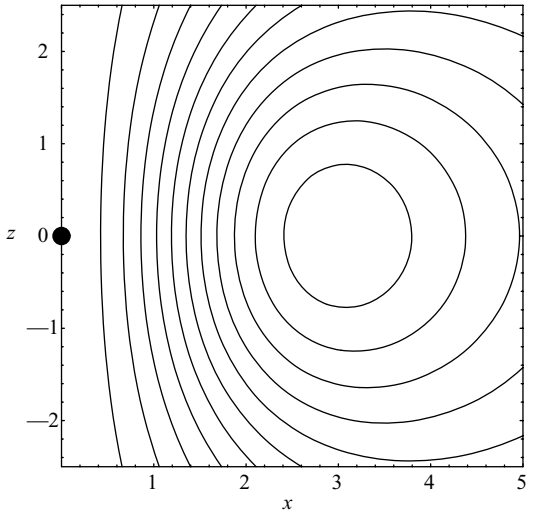

FIGURE 1. The streamlines for the flow corresponding to the velocity field given by (8) at time $t = 1$ for impulse $S = 1$ and kinematic viscosity $\nu = 1$.

The stream function representation of the flow field is almost as simple as the one given in (3), but it has the advantage of the property (10) which allows easy plotting of the streamlines. Also it is immediately obvious from (8) that $\boldsymbol{\nabla}\cdot\boldsymbol{v}_s = 0$. In figure 1 we plot the streamlines at a particular value of time, as given by the contours of constant stream function $\Psi_s(\boldsymbol{r}, t)$. It is evident that the flow is characterized by an expanding vortex ring, as for a suddenly accelerated sphere (Felderhof 2007*b*). Because in (1) we use a monopole approximation, the scaling flow pattern is independent of the slip coefficient.

The kinetic energy of the flow field is defined by

$$\mathscr{T}_s(t) = \frac{1}{2}\rho \int \boldsymbol{v}_s^2(\boldsymbol{r}, t)\, \mathrm{d}\boldsymbol{r}. \tag{15}$$

From (2) one finds

$$\mathscr{T}_s(t) = \left(\frac{S}{4\pi\eta}\right)^2 \frac{1}{3}\rho\sqrt{\frac{\pi\nu}{2t^3}} \qquad \text{for } t > 0. \tag{16}$$

This shows a characteristic power-law decay.

The fluid momentum is not properly defined, since the integral over all space of the fluid velocity does not converge absolutely. With the integration prescription that the integral over angles is performed first it takes the value

$$\rho \int' \boldsymbol{v}_s(\boldsymbol{r}, t)\, \mathrm{d}\boldsymbol{r} = \tfrac{2}{3}\boldsymbol{S}, \tag{17}$$

where the prime on the integral sign is a reminder of the prescription. It has been argued that at $t = 0$ one-third of the imparted momentum is transported to infinity by sound waves (Cichocki & Felderhof 2000). For finite sound velocity the integral converges absolutely to value $\boldsymbol{S}$, and no integration prescription is needed (Felderhof 2007*c*). The power law decay in (16) follows qualitatively from the observation that at time t the characteristic length of momentum diffusion is $\lambda(t) = \sqrt{4\nu t}$, and that

according to the conservation law (17) the velocity in a sphere of volume λ^3 centred at the origin decays in proportion to $t^{-3/2}$.

The long-time behaviour of the velocity of the accelerated sphere is independent of its mass, its radius, and of the slip coefficient. The scaling velocity may be found from the behaviour of the Green function at the origin (Cichocki & Felderhof 2000). It is given by

$$\boldsymbol{U}_s(t) = \frac{1}{12\rho(\pi\nu t)^{3/2}}\boldsymbol{S}. \tag{18}$$

The physical reason for the independence of mass, radius, and slip coefficient is that at long times the fluid flow pattern is given by the universal scaling form derived above. We define the corresponding scaling mass $m_s(t)$ from the identity

$$\mathscr{T}_s(t) = \tfrac{1}{2}m_s(t)\boldsymbol{U}_s(t)^2. \tag{19}$$

From (16) and (18) we find

$$m_s(t) = 3\sqrt{2}\rho(\pi\nu t)^{3/2}. \tag{20}$$

The generalized momentum

$$\boldsymbol{P}_{gs} = \frac{\partial \mathscr{T}_s}{\partial \boldsymbol{U}_s} = m_s(t)\boldsymbol{U}_s(t) \tag{21}$$

is conserved, and takes the value

$$\boldsymbol{P}_{gs} = \frac{1}{2\sqrt{2}}\boldsymbol{S}. \tag{22}$$

Note that this differs from the value given by (17).

3. Energy of flow about an accelerated sphere

The flow field around a sphere accelerated by a force $\boldsymbol{E}(t)$ applied at the centre and with mixed slip–stick boundary conditions applied at the surface of the sphere can be studied by the method of Fourier transform (Albano, Bedeaux & Mazur 1975; Felderhof 1976; Felderhof & Jones 1986). Owing to the applied force the sphere acquires a velocity $\boldsymbol{U}(t)$, which can be evaluated from the frequency-dependent admittance (Felderhof 1991). In the rest frame of the sphere the Navier–Stokes equations for the flow field $\boldsymbol{v}'(\boldsymbol{r}, t)$ are

$$\rho\left[\frac{\partial \boldsymbol{v}'}{\partial t} + (\boldsymbol{v}'\cdot\nabla)\boldsymbol{v}'\right] = \eta\nabla^2\boldsymbol{v}' - \nabla p - \rho\frac{\mathrm{d}\boldsymbol{U}}{\mathrm{d}t}, \qquad \nabla\cdot\boldsymbol{v}' = 0. \tag{23}$$

The flow field $\boldsymbol{v}'(\boldsymbol{r}, t)$ in the rest frame and the flow field $\boldsymbol{u}(\boldsymbol{r}_0, t)$ in the laboratory frame are related by

$$\boldsymbol{v}'(\boldsymbol{r}, t) = \boldsymbol{u}(\boldsymbol{r}_0, t) - \boldsymbol{U}(t), \tag{24}$$

and the coordinates in the two frames are related by

$$\boldsymbol{r} = \boldsymbol{r}_0 - \int_0^t \boldsymbol{U}(t')\,\mathrm{d}t'. \tag{25}$$

We write the solution of (23) as

$$\boldsymbol{v}'(\boldsymbol{r}, t) = -\boldsymbol{U}(t) + \boldsymbol{v}(\boldsymbol{r}, t), \tag{26}$$

with the field $\boldsymbol{v}(\boldsymbol{r}, t)$ tending to zero as $r \to \infty$. Substituting into (23) and linearizing for small velocity $\boldsymbol{U}(t)$ one finds that $\boldsymbol{v}(\boldsymbol{r}, t)$ satisfies the linear equations

$$\rho \frac{\partial \boldsymbol{v}}{\partial t} = \eta \nabla^2 \boldsymbol{v} - \nabla p, \qquad \nabla \cdot \boldsymbol{v} = 0 \qquad \text{for } r > a. \tag{27}$$

These are the equations solved by a Fourier transform with respect to time in Albano *et al.* (1975).

It follows in particular from (24) and (26) that

$$\int_{\overline{V_0(t)}} \boldsymbol{u}(\boldsymbol{r}_0, t)^2 \, \mathrm{d}\boldsymbol{r}_0 = \int_{r>a} \boldsymbol{v}(\boldsymbol{r}, t)^2 \, \mathrm{d}\boldsymbol{r}, \tag{28}$$

where $\overline{V_0(t)}$ is the volume complementary to the moving sphere. Therefore the energy in the laboratory frame can be calculated from the solution $\boldsymbol{v}(\boldsymbol{r}, t)$ in the rest frame. The time-dependent flow field for a delta-function force pulse and for a constant force acting during a time interval T was found in Felderhof (2007*a*,*b*).

We consider first a delta-function pulse corresponding to an applied force $\boldsymbol{E}(t) = \boldsymbol{S}\delta(t)$. The resulting sphere velocity in the laboratory frame is

$$\boldsymbol{U}(t) = \frac{\boldsymbol{S}}{m^*} F(t), \tag{29}$$

where $m^* = m_p + \frac{1}{2} m_f$ is the effective mass (Lighthill 1986), with mass $m_f = \frac{4}{3}\pi\rho a^3$, and $F(t)$ is the normalized velocity relaxation function

$$F(t) = \sum_{j=1}^{3} A_j x_j w(-\mathrm{i} q_j \sqrt{\nu t}), \tag{30}$$

where $w(z)$ is the w-function (Abramowitz & Stegun 1965), and $q_j = x_j/a$. The three values $\{x_j\}$ are the zeros of a cubic derived from the frequency-dependent impedance, and the amplitudes $\{A_j\}$ are corresponding residues (see equations (97)–(102) of Felderhof 2007*b*). The initial value of the relaxation function is $F(0+) = 1$.

The kinetic energy of the fluid is defined by

$$\mathscr{T}_f(t) = \frac{1}{2} \int_{r>a} \rho \boldsymbol{v}(\boldsymbol{r}, t)^2 \, \mathrm{d}\boldsymbol{r}. \tag{31}$$

We have not found an analytic form for the energy $\mathscr{T}_f(t)$. With a stream function representation analogous to (8) it can be expressed as a radial integral,

$$\mathscr{T}_f(t) = \frac{4\pi}{3} \rho \int_a^\infty \left[\left(\frac{\partial \chi(r, t)}{\partial r} \right)^2 + \frac{2}{r} \chi(r, t)^2 \right] \mathrm{d}r, \tag{32}$$

where the radial function $\chi(r, t)$ can be written as the sum of a pressure part and a viscous part. The pressure part is in normalized form (Felderhof 2007*b*)

$$\psi_{P*}(r, t) = \frac{Q_F(t)}{r}, \tag{33}$$

with dipole strength

$$Q_F(t) = \tfrac{1}{2}(1 - 3Z) a^3 F(t) + \tfrac{3}{2} Z a^3, \tag{34}$$

where $Z = 2m^*/9m_f$. The expanding viscous boundary layer is described by a second scalar function $\psi_{V*}(r, t)$, given explicitly by equation (40) of Felderhof (2007*a*). The

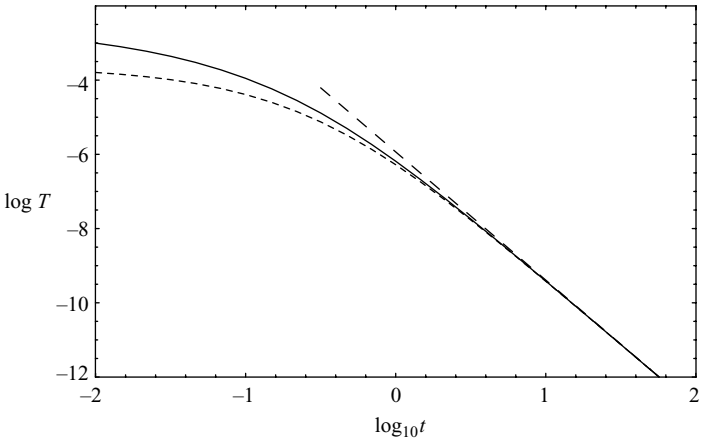

FIGURE 2. $\log \mathscr{T}_f(t)$ after a sudden impulse $S = 1$, as given by (32), as a function of $\log_{10} t$ for a sphere with $Z = 2m^*/9m_f = 1/3$ (short dashes). We compare with the total energy $\log \mathscr{T}(t)$, as given by (39) (solid curve), and with the scaling expression given by (16) (long dashes).

scalar function to be used in (32) is

$$\chi(r, t) = \frac{S}{m^*}[\psi_{P*}(r, t) + \psi_{V*}(r, t)]. \tag{35}$$

At short times the viscous part vanishes and the flow is irrotational. At long times the flow is close to that given by the Green function in § 2. At large distance the flow becomes dipolar. We note that $6\pi\rho Z a^3 = m^*$, showing that the long-time value of the dipole strength agrees with that of the scaling flow.

From (32)–(34) one finds for the initial value of the fluid kinetic energy

$$\mathscr{T}_f(0+) = \tfrac{1}{4} m_f \left(\frac{S}{m^*}\right)^2 = \tfrac{1}{4} m_f U(0+)^2, \tag{36}$$

in agreement with potential flow theory (Lighthill 1986). At long times we expect

$$\mathscr{T}_f(t) \approx \mathscr{T}_s(t) \qquad \text{as } t \to \infty, \tag{37}$$

with $\mathscr{T}_s(t)$ given by (16). In figure 2 we show the behaviour of the energy as a function of time for a sphere with $Z = 1/3$ and for stick boundary conditions. In all figures we use units such that the sphere has radius $a = 1$ and the fluid has mass density $\rho = 1$ and shear viscosity $\eta = 1$.

The total kinetic energy of sphere and fluid is

$$\mathscr{T}(t) = \mathscr{T}_p(t) + \mathscr{T}_f(t) = \tfrac{1}{2} m_p \boldsymbol{U}(t)^2 + \mathscr{T}_f(t). \tag{38}$$

This can be used to define the time-dependent virtual mass $m_v(t)$ by

$$\mathscr{T}(t) = \tfrac{1}{2} m_v(t) \boldsymbol{U}(t)^2. \tag{39}$$

At short times

$$m_v(0+) = m_p + \tfrac{1}{2} m_f = m^*, \tag{40}$$

where $m_a = \frac{1}{2} m_f$ is the added mass of potential flow theory (Lighthill 1986). At long times the virtual mass shows scaling behaviour,

$$m_v(t) \approx m_s(t) \qquad \text{as } t \to \infty, \tag{41}$$

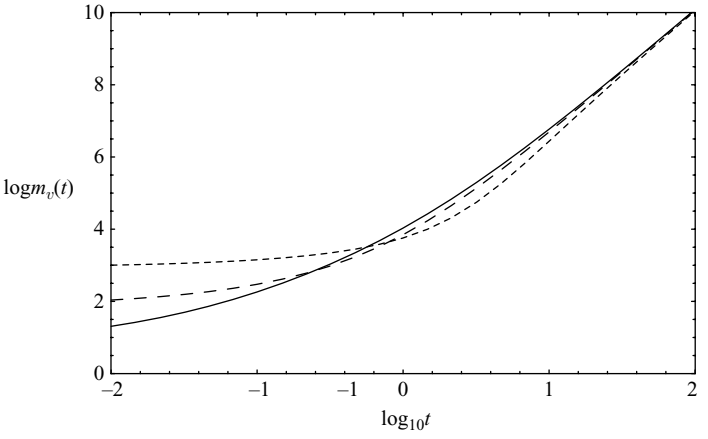

FIGURE 3. $\log m_v(t)$ after a sudden impulse, where $m_v(t)$ is the virtual mass defined in (40), as a function of $\log_{10} t$ for a sphere with $Z = 2m^*/9m_f = 1/9$ (solid curve), $Z = 1/3$ (long dashes), and $Z = 1$ (short dashes).

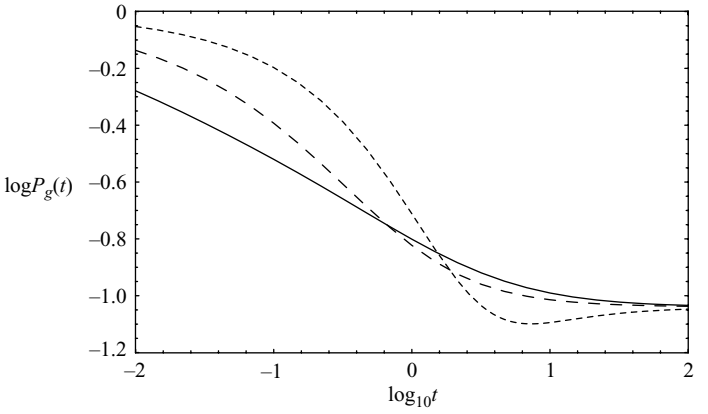

FIGURE 4. $\log m_v(t)F(t)/m^*$ after a sudden impulse $S = 1$ as a function of $\log_{10} t$ for a sphere with $Z = 2m^*/9m_f = 1/9$ (solid curve), $Z = 1/3$ (long dashes), and $Z = 1$ (short dashes).

independent of the mass m_p, the radius a, and the slip parameter. In figure 3 we show the time-dependence of the virtual mass for three values of the parameter Z and for stick boundary conditions. From (18) and (29) it follows that the long-time behaviour of the velocity relaxation function is given by

$$F(t) \approx \frac{m^*}{12}\sqrt{\rho}(\pi\eta t)^{-3/2} = \frac{1}{2\sqrt{2}}\frac{m^*}{m_s(t)} \qquad \text{as } t \to \infty. \tag{42}$$

In figure 4 we plot the behaviour of the product $m_v(t)F(t)/m^*$ for three values of Z and stick boundary conditions. This shows that the generalized momentum

$$\boldsymbol{P}_g(t) = \frac{\partial \mathscr{T}}{\partial \boldsymbol{U}} = m_v(t)\boldsymbol{U}(t) \tag{43}$$

is time-dependent. The initial value is $\boldsymbol{P}_g(0+) = \boldsymbol{S}$, and in the scaling limit $\boldsymbol{P}_{gs} = \boldsymbol{S}/2\sqrt{2}$, as in (22). The time-dependence is caused by dissipation.

4. Constant applied force

Next we consider a constant force applied to the centre of the sphere and starting at time $t = 0$,

$$\boldsymbol{E}(t) = \boldsymbol{E}_0 H(t), \tag{44}$$

where $H(t)$ is the Heaviside step-function. We denote the corresponding sphere velocity as $\overline{\boldsymbol{U}}(t)$ and the position of the centre of the sphere in the laboratory frame as

$$\boldsymbol{R}_0(t) = \int_0^t \overline{\boldsymbol{U}}(t')\,\mathrm{d}t'. \tag{45}$$

We take the position in the rest frame to coincide with the origin. For large t the position $\boldsymbol{R}_0(t)$ can be far from the origin of the laboratory frame.

In particular we consider the kinetic energy of the flow field at time t. For sufficiently large t this can again to a good approximation be found from the Green function. Thus instead of the scalar function in (12) we consider its time integral

$$\overline{\chi}_s(r,t) = \int_0^t \chi_s(r,t')\,\mathrm{d}t' = \frac{r}{2}\mathrm{erfc}\left(\frac{r}{\sqrt{4\nu t}}\right) + t\,\chi_s(r,t). \tag{46}$$

This provides the flow disturbance in the rest frame at time t. The flow $\overline{\boldsymbol{v}}_s(\boldsymbol{r},t)$ is given by

$$\overline{\boldsymbol{v}}_s(\boldsymbol{r},t) = \frac{E_0}{4\pi\eta}\nabla\times\left(\frac{1}{r}\overline{\chi}_s(r,t)\sin\theta\;\boldsymbol{e}_\varphi\right). \tag{47}$$

We write

$$\overline{\chi}_s(r,t) = \tfrac{1}{2}r + \Delta\chi_s(r,t). \tag{48}$$

The first term corresponds to the steady-state Oseen tensor, which is singular at $r = 0$. The second term corresponds to a flow which is regular at $r = 0$. From the value at $r = 0$ we find the scaling velocity

$$\Delta\overline{\boldsymbol{U}}_s(t) = -\frac{\boldsymbol{E}_0}{6\pi^{3/2}\eta\sqrt{\nu t}}. \tag{49}$$

This corresponds to the long-time correction to the terminal velocity $\boldsymbol{E}_0/\zeta_0$ of the sphere (Felderhof 2007*a*), where ζ_0 is the steady-state friction coefficient. The correction term is independent of the mass and size of the sphere and of the slip parameter (in equations (17) and (18) of Felderhof (2007*a*) a factor $\sqrt{\pi}$ is missing in the denominator). The complete expression for the velocity of the sphere is

$$\overline{\boldsymbol{U}}(t) = \frac{\boldsymbol{E}_0}{m^*}G(t) \tag{50}$$

with response function $G(t)$ given by

$$G(t) = \int_0^t F(t')\,\mathrm{d}t'. \tag{51}$$

The expression for the integral is given in Felderhof (2007*a*), equations (10), (11). The sphere speeds up, starting with initial acceleration $\boldsymbol{E}_0/m^*$, and reaching the Stokes velocity $\boldsymbol{E}_0/\zeta_0$.

The kinetic energy of the disturbance corresponding to (47) is

$$\overline{\mathscr{T}}_s(t) = \left(\frac{E_0}{4\pi\eta}\right)^2\frac{8}{3}(2-\sqrt{2})\rho\sqrt{\pi\nu t}. \tag{52}$$

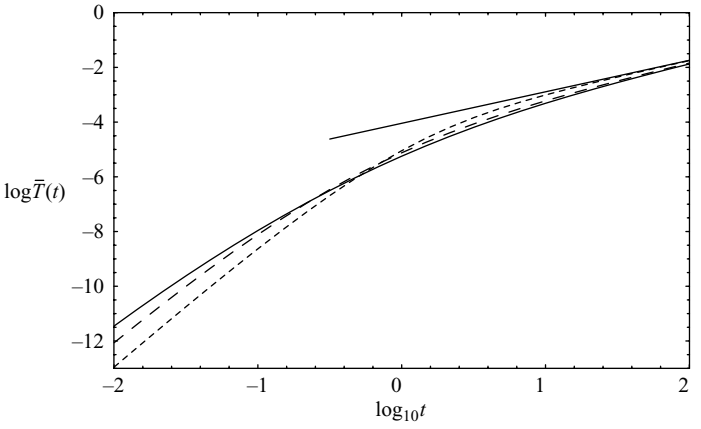

FIGURE 5. $\log\overline{\mathscr{T}}(t)$ for applied force $E_0 = 1$ as a function of $\log_{10}t$ for a sphere with $Z = 2m^*/9m_f = 1/9$ (solid curve), $Z = 1/3$ (long dashes), and $Z = 1$ (short dashes). We compare with the scaling expression given by (52) (solid straight line).

This can be used to define the scaling mass $\overline{m}_s(t)$ by

$$\overline{\mathscr{T}}_s(t) = \tfrac{1}{2}\overline{m}_s(t)\big(\Delta\overline{\boldsymbol{U}}_s(t)\big)^2, \tag{53}$$

which yields the expression

$$\overline{m}_s(t) = 12(2-\sqrt{2})\rho(\pi\nu t)^{3/2}. \tag{54}$$

The numerical value of the coefficient is $12(2-\sqrt{2}) = 7.029$. This is to be compared with the value $3\sqrt{2} = 4.243$ in (20).

Corresponding to (52) we expect that for the flow about a sphere the energy of the flow disturbance vanishes at $t = 0$, and after transient effects grows in the same manner in proportion to $\sqrt{t}$ at long times. The total energy at time t is

$$\overline{\mathscr{T}}(t) = \overline{\mathscr{T}}_p(t) + \overline{\mathscr{T}}_f(t) = \tfrac{1}{2}m_p\overline{\boldsymbol{U}}(t)^2 + \overline{\mathscr{T}}_f(t). \tag{55}$$

This can be used to define the time-dependent virtual mass $\overline{m}_v(t)$ by

$$\overline{\mathscr{T}}(t) = \tfrac{1}{2}\overline{m}_v(t)\left[\overline{\boldsymbol{U}}(t) - \frac{\boldsymbol{E}_0}{\zeta_0}\right]^2. \tag{56}$$

Scaling behaviour implies $\overline{m}_v(t) \approx \overline{m}_s(t)$ at long times. In figure 5 we plot the total energy $\overline{\mathscr{T}}(t)$ as a function of time for three values of Z and stick boundary conditions, and compare with the scaling expression (52).

5. Pair interaction

We consider two identical spheres under the influence of a constant force $\boldsymbol{E}_0$ starting at time $t = 0$. Initially the spheres are at rest at positions $\boldsymbol{R}_1(0)$, $\boldsymbol{R}_2(0)$ with distance vector $\boldsymbol{R}(0) = \boldsymbol{R}_2(0) - \boldsymbol{R}_1(0)$. If the distance is sufficiently large compared with the radius a we expect that hydrodynamic interactions between the two spheres may be evaluated from the scaling flow patterns of both spheres. This suggests that to a good approximation the rate of change of both positions is given by the equations

of transient Stokesian dynamics

$$\left.\begin{aligned}\frac{\mathrm{d}\boldsymbol{R}_1}{\mathrm{d}t} &= \overline{\boldsymbol{U}}(t) + \frac{1}{4\pi\eta}\overline{\boldsymbol{T}}(\boldsymbol{R}_1(t) - \boldsymbol{R}_2(t), t)\cdot\boldsymbol{E}_0,\\ \frac{\mathrm{d}\boldsymbol{R}_2}{\mathrm{d}t} &= \overline{\boldsymbol{U}}(t) + \frac{1}{4\pi\eta}\overline{\boldsymbol{T}}(\boldsymbol{R}_2(t) - \boldsymbol{R}_1(t), t)\cdot\boldsymbol{E}_0,\end{aligned}\right\} \tag{57}$$

with the tensor

$$\overline{\boldsymbol{T}}(\boldsymbol{r}, t) = \int_0^t \boldsymbol{T}(\boldsymbol{r}, t')\,\mathrm{d}t'. \tag{58}$$

The flow in (47) can be expressed as

$$\overline{\boldsymbol{v}}_s(\boldsymbol{r}, t) = \frac{1}{4\pi\eta}\overline{\boldsymbol{T}}(\boldsymbol{r}, t)\cdot\boldsymbol{E}_0. \tag{59}$$

From (3) we find the expression

$$\overline{\boldsymbol{T}}(\boldsymbol{r}, t) = \mathbf{1}\frac{\mathrm{erfc}(r/\lambda)}{r} + \nabla\nabla\left[\frac{\nu t}{r}\mathrm{erf}\frac{r}{\lambda} + \sqrt{\frac{\nu t}{\pi}}e^{-r^2/\lambda^2} - \frac{r}{2}\mathrm{erfc}\left(\frac{r}{\lambda}\right)\right], \tag{60}$$

with $\lambda = \sqrt{4\nu t}$. Since $\overline{\boldsymbol{T}}(-\boldsymbol{r}, t) = \overline{\boldsymbol{T}}(\boldsymbol{r}, t)$, it follows from these equations that the distance vector $\boldsymbol{R} = \boldsymbol{R}_2(t) - \boldsymbol{R}_1(t)$ is independent of time.

We suggest in the following that the distance vector does change owing to inertial effects. We perform a calculation of the kinetic energy of the flow in the scaling regime. It turns out that the energy depends on the distance vector owing to interference of the two flow patterns. It follows from non-equilibrium thermodynamics that this results in a force between the two spheres.

Since to lowest order the relative distance vector is constant, we can use a coordinate system in which both spheres are at rest at time t. The origin of the rest frame moves with respect to the laboratory frame with a velocity given by the right-hand side of (57). The total kinetic energy of the flow disturbance in the scaling regime takes the form

$$\overline{\mathscr{T}}_s(\boldsymbol{R}, t) = \overline{\mathscr{T}}_{11s}(t) + \overline{\mathscr{T}}_{22s}(t) + \overline{\mathscr{T}}_{12s}(\boldsymbol{R}, t), \tag{61}$$

where the first two terms are equal and given by the single-sphere expression (52), and the last term takes the value

$$\overline{\mathscr{T}}_{12s}(\boldsymbol{R}, t) = \rho\int \overline{\boldsymbol{v}}_s(\boldsymbol{r}, t)\cdot\overline{\boldsymbol{v}}_s(\boldsymbol{r} - \boldsymbol{R}, t)\,\mathrm{d}\boldsymbol{r}, \tag{62}$$

with flow $\overline{\boldsymbol{v}}_s(\boldsymbol{r}, t)$ given by (59). We calculate the integral by use of Parseval's theorem. Thus we define the spatial Fourier transform

$$\hat{\overline{\boldsymbol{v}}}_s(\boldsymbol{k}, t) = \int \exp(-\mathrm{i}\boldsymbol{k}\cdot\boldsymbol{r})\overline{\boldsymbol{v}}_s(\boldsymbol{r}, t)\,\mathrm{d}\boldsymbol{r}. \tag{63}$$

Then the integral in (62) is given by

$$\overline{\mathscr{T}}_{12s}(\boldsymbol{R}, t) = \frac{\rho}{8\pi^3}\int |\hat{\overline{\boldsymbol{v}}}_s(\boldsymbol{k}, t)|^2\exp(\mathrm{i}\boldsymbol{k}\cdot\boldsymbol{R})\,\mathrm{d}\boldsymbol{k}. \tag{64}$$

The Fourier transform of the Green function is given by

$$\hat{\boldsymbol{T}}(\boldsymbol{k}, t) = 4\pi\nu(\mathbf{1} - \hat{\boldsymbol{k}}\hat{\boldsymbol{k}})\mathrm{e}^{-k^2\lambda^2/4}. \tag{65}$$

The Fourier transform of the time-integral is

$$\hat{\overline{\boldsymbol{T}}}(\boldsymbol{k}, t) = 4\pi(\mathbf{1} - \hat{\boldsymbol{k}}\hat{\boldsymbol{k}})\frac{1 - \mathrm{e}^{-k^2\lambda^2/4}}{k^2}. \tag{66}$$

Hence

$$\overline{\mathscr{T}}_{12s}(\boldsymbol{R},t)=\frac{\rho}{8\pi^3\eta^2}\int \boldsymbol{E}_0\cdot(\mathbf{1}-\hat{\boldsymbol{k}}\hat{\boldsymbol{k}})\cdot\boldsymbol{E}_0\frac{(1-\mathrm{e}^{-k^2\lambda^2/4})^2}{k^4}\exp(\mathrm{i}\boldsymbol{k}\cdot\boldsymbol{R})\,\mathrm{d}\boldsymbol{k}. \tag{67}$$

This results in

$$\overline{\mathscr{T}}_{12s}(\boldsymbol{R},t)=\frac{\lambda\rho}{8\pi^{3/2}\eta^2}\boldsymbol{E}_0\cdot\boldsymbol{U}(\boldsymbol{R},t)\cdot\boldsymbol{E}_0, \tag{68}$$

with tensor

$$\boldsymbol{U}(\boldsymbol{R},t)=X\left(\frac{R}{\lambda}\right)\mathbf{1}+\lambda^2\frac{\partial^2}{\partial\boldsymbol{R}\partial\boldsymbol{R}}Y\left(\frac{R}{\lambda}\right), \tag{69}$$

where the scaling function $X(s)$ with $s=R/\lambda$ is given by

$$X(s)=2\mathrm{e}^{-s^2}-\sqrt{2}\mathrm{e}^{-s^2/2}-\sqrt{\pi}s+\sqrt{\pi}\left(2s+\frac{1}{s}\right)\mathrm{erf}\,s-\sqrt{\pi}\left(s+\frac{1}{s}\right)\mathrm{erf}\frac{s}{\sqrt{2}}, \tag{70}$$

and the function $Y(s)$ is given by

$$\begin{aligned}Y(s)=\frac{1}{12}\big(\sqrt{\pi}s^3-(5+2s^2)\mathrm{e}^{-s^2}+\sqrt{2}(5+s^2)\mathrm{e}^{-s^2/2}\big)-\frac{\sqrt{\pi}}{24s}\big(3+12s^2+4s^4\big)\mathrm{erf}\,s\\+\frac{\sqrt{\pi}}{12s}\big(3+6s^2+s^4\big)\mathrm{erf}\frac{s}{\sqrt{2}}.\end{aligned} \tag{71}$$

At $s=0$ the functions take the values

$$X(0)=2(2-\sqrt{2}),\qquad Y(0)=\tfrac{2}{3}(\sqrt{2}-1). \tag{72}$$

We note that for an isotropic function $f(R)$

$$\boldsymbol{E}_0\cdot\frac{\partial^2 f(R)}{\partial\boldsymbol{R}\partial\boldsymbol{R}}\cdot\boldsymbol{E}_0=E_0^2\left[\frac{\mathrm{d}^2 f}{\mathrm{d}R^2}\cos^2\Theta+\frac{1}{R}\frac{\mathrm{d}f}{\mathrm{d}R}\sin^2\Theta\right], \tag{73}$$

where Θ is the angle between $\boldsymbol{R}$ and $\boldsymbol{E}_0$. Hence we find that the interaction energy can be expressed as the sum of an isotropic and an anisotropic part,

$$\overline{\mathscr{T}}_{12s}(\boldsymbol{R},t)=\frac{\lambda\rho E_0^2}{8\pi^{3/2}\eta^2}[V(s)+A(s)P_2(\cos\Theta)], \tag{74}$$

where

$$V(s)=X(s)+\frac{1}{3}Y''(s)+\frac{2}{3s}Y'(s),\qquad A(s)=\frac{2}{3}Y''(s)-\frac{2}{3s}Y'(s). \tag{75}$$

The isotropic part is given by

$$V(s)=\frac{2}{3}\big(2\mathrm{e}^{-s^2}-\sqrt{2}\mathrm{e}^{-s^2/2}\big)-\frac{2\sqrt{\pi}}{3}\left(s-\left(2s+\frac{1}{s}\right)\mathrm{erf}\,s+\left(s+\frac{1}{s}\right)\mathrm{erf}\frac{s}{\sqrt{2}}\right), \tag{76}$$

and the anisotropic part by

$$\begin{aligned}A(s)=\frac{1}{6s^2}\left((3-2s^2)\mathrm{e}^{-s^2}-(3-s^2)\sqrt{2}\mathrm{e}^{-s^2/2}\right)\\+\frac{\sqrt{\pi}}{12s^3}\left(2s^4-(3-4s^2+4s^4)\mathrm{erf}\,s+2(3-2s^2+s^4)\mathrm{erf}\frac{s}{\sqrt{2}}\right).\end{aligned} \tag{77}$$

At small distance

$$V(s)=\frac{4}{3}(2-\sqrt{2})+O(s),\qquad A(s)=\frac{\sqrt{\pi}}{6}s+O(s^2). \tag{78}$$

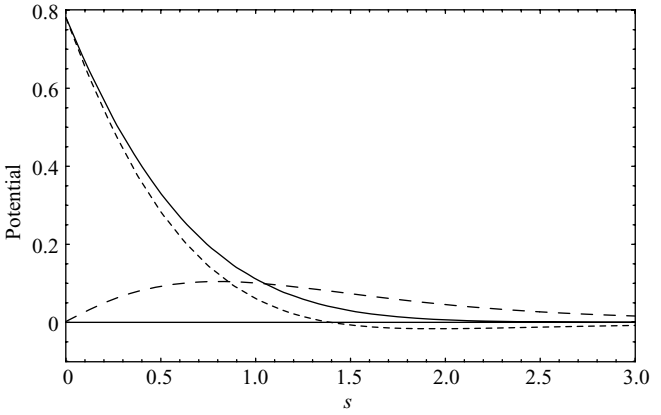

FIGURE 6. The isotropic potential $V(s)$ (solid curve), the anisotropic potential $A(s)$ (long dashes), and of the combination $V(s) - \frac{1}{2}A(s)$ relevant for $\Theta = \pi/2$ (short dashes).

The first equality is in agreement with the value of the interaction energy at $\boldsymbol{R} = \boldsymbol{0}$, as given by (52), since it follows from (62) that

$$\overline{\mathscr{T}}_{12s}(\boldsymbol{0}, t) = 2\overline{\mathscr{T}}_{s}(t). \tag{79}$$

At long distance the isotropic term $V(s)$ tends to zero rapidly, but the anisotropic term $A(s)$ tends to $\sqrt{\pi}/(4s^3)$, so that the interaction given by (74) is dipolar at long range. In figure 6 we plot the scaling functions $V(s)$ and $A(s)$, as well as the function $V(s) - \frac{1}{2}A(s)$ corresponding to $\Theta = \pi/2$. Remarkably, the latter function shows a minimum. It has a zero at $s_0 = 1.393$, and a minimum at $s_m = 1.944$, where the function takes the value $V(s_m) - \frac{1}{2}A(s_m) = -0.01645$. In figure 7 we show a contour plot of the quantity $V(s) + A(s)P_2(\cos\Theta)$.

The kinetic energy $\overline{\mathscr{T}}(\boldsymbol{R}, t)$ makes a distance-dependent contribution to the non-equilibrium free energy of the entire system. We argue on the basis of a general principle of irreversible thermodynamics (Einstein 1906; Onsager 1931) that the rate of change of the distance vector is proportional to the gradient of the non-equilibrium free energy with respect to $\boldsymbol{R}$. In the long-time limit and for large distance the proportionality factor is given by just the steady-state single-sphere mobility. On these grounds we replace (57) by

$$\left.\begin{aligned} \frac{\mathrm{d}\boldsymbol{R}_1}{\mathrm{d}t} &= \overline{\boldsymbol{U}}(t) + \frac{1}{4\pi\eta}\overline{\boldsymbol{T}}(\boldsymbol{R}_1 - \boldsymbol{R}_2, t)\cdot\boldsymbol{E}_0 - \mu_0\frac{\partial\overline{\mathscr{T}}_{12s}(\boldsymbol{R}_1 - \boldsymbol{R}_2, t)}{\partial\boldsymbol{R}_1}, \\ \frac{\mathrm{d}\boldsymbol{R}_2}{\mathrm{d}t} &= \overline{\boldsymbol{U}}(t) + \frac{1}{4\pi\eta}\overline{\boldsymbol{T}}(\boldsymbol{R}_2 - \boldsymbol{R}_1, t)\cdot\boldsymbol{E}_0 - \mu_0\frac{\partial\overline{\mathscr{T}}_{12s}(\boldsymbol{R}_1 - \boldsymbol{R}_2, t)}{\partial\boldsymbol{R}_2}, \end{aligned}\right\} \tag{80}$$

where $\mu_0 = 1/\zeta_0$. Subtracting the two equations one sees that the inertial force causes a change of the relative distance vector. Qualitatively the nature of the driving force corresponds with the experiments by Jayaweera *et al.* (1964). The steady-state friction coefficient ζ_0 depends on the slip coefficient. It is given by $\zeta_0 = 6\pi(1-\xi)\eta a$, with slip parameter $\xi = 0$ for stick boundary conditions and $\xi = 1/3$ for perfect slip (Felderhof 1976).

More generally, for N settling spheres the equations of motion are

$$\frac{\mathrm{d}\boldsymbol{R}_j}{\mathrm{d}t} = \overline{\boldsymbol{U}}(t) + \frac{1}{4\pi\eta}\sum_{k\neq j}^{N}\overline{\boldsymbol{T}}(\boldsymbol{R}_j - \boldsymbol{R}_k, t)\cdot\boldsymbol{E}_0 - \mu_0\sum_{k\neq j}^{N}\frac{\partial\overline{\mathscr{T}}_{12s}(\boldsymbol{R}_j - \boldsymbol{R}_k, t)}{\partial\boldsymbol{R}_j}, \qquad j = 1, \ldots, N. \tag{81}$$

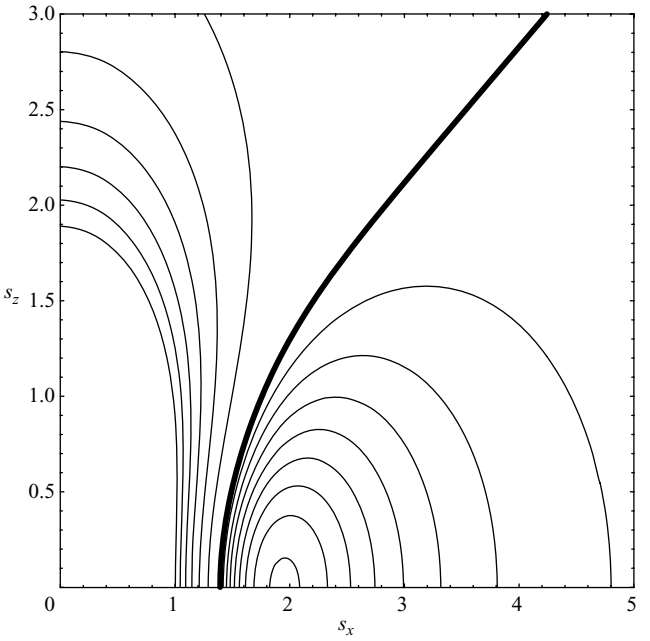

FIGURE 7. Contour plot of the potential $V(s) + A(s)P_2(\cos\Theta)$. The thick line corresponds to vanishing potential. To the left of the line the potential is positive, to the right it is negative.

Since the hydrodynamic interaction is limited to a single propagator, many-body effects are neglected and only the simplified pair interaction is taken into account. The explicit expressions for the pair interaction derived above allow a study of the dynamics of N spheres by numerical solution of these equations. The results should be compared with computer simulation and experiment. Both pair interaction terms are dipolar at long range.

We compare the pair interaction derived above with the effective interaction force found in the theory of irrotational flow. For simplicity we consider only the behaviour at large distance. According to classical results described by Lamb (1932) the distance dependence of the kinetic energy gives rise to a force between two moving spheres. The force is repulsive when the two velocity vectors are in the same direction along the line of centres, and attractive when the two velocity vectors are in the same direction perpendicular to the line of centres. The results can be summarized in an expression for the kinetic energy valid at large distance. For two spheres of radii a and b this becomes

$$\mathscr{T}_{irr} = \tfrac{1}{2}m_1^*\boldsymbol{U}_1^2 + \tfrac{1}{2}m_2^*\boldsymbol{U}_2^2 - \pi\rho a^3b^3\boldsymbol{U}_1\cdot\frac{-\mathbf{1}+3\hat{\boldsymbol{R}}\hat{\boldsymbol{R}}}{R^3}\cdot\boldsymbol{U}_2, \tag{82}$$

where m_1^* and m_2^* are the two effective masses. The vector form presented in (82) is new. The acceleration of the two spheres is calculated from the kinetic energy by use of Lagrange's equations of motion. For equal velocities the dipolar interaction term can be expressed as

$$\mathscr{T}_{irr12} = -2\pi\rho a^3b^3\frac{U_1^2}{R^3}P_2(\cos\Theta'), \tag{83}$$

where Θ' is the angle between $\boldsymbol{U}_1$ and $\boldsymbol{R}$. This can be compared with the large-distance behaviour of the interaction energy in (83), which is given by

$$\overline{\mathscr{T}}_{12s}^{dip}(\boldsymbol{R}, t) = \frac{\lambda^4 \rho E_0^2}{32\pi\eta^2 R^3} P_2(\cos\Theta). \tag{84}$$

Thus the two interaction energies are of opposite sign, if to lowest order we neglect the interactions in (80) and identify Θ and Θ'. Nonetheless, because in the case of (83) the accelerations are calculated by use of Lagrange's equations, and in the case of (84) the velocities are calculated from the negative gradient with respect to the distance vector, both expressions lead to qualitatively the same result. In the case of (84) the two spheres tend to move apart when the applied force is directed along the line of centres, and they tend to move together when the applied force is directed perpendicular to the line of centres. Note that the amplitude in (84) increases with time as t^2.

The solution of the pair equations of motion (80) is best performed in terms of centre-of-mass and relative coordinates. The equation of motion for the relative coordinate vector becomes in the scaling regime

$$\frac{\mathrm{d}\boldsymbol{R}}{\mathrm{d}t} = -2\mu_0 \frac{\partial \overline{\mathscr{T}}_{12s}(\boldsymbol{R}, t)}{\partial \boldsymbol{R}}. \tag{85}$$

For the situation considered by Jayaweera *et al.* (1964), where the two spheres start from rest at positions $\boldsymbol{R}_1(0)$ and $\boldsymbol{R}_2(0)$, one can first solve numerically up to a time t_0 when transient effects are past and the scaling regime has been reached. In the scaling regime it is convenient to use scaled coordinates. The relative distance vector becomes $\boldsymbol{R} = \lambda \boldsymbol{s}$. We take out the factor λ in (74) by defining $\hat{\overline{\mathscr{T}}}_{12s} = \overline{\mathscr{T}}_{12s}/\lambda$. Then the transformed equation of motion for the vector $\boldsymbol{s}$ becomes

$$\frac{\mathrm{d}\boldsymbol{s}}{\mathrm{d}u} = -\frac{\partial}{\partial \boldsymbol{s}}\left(\frac{s^2}{u} + \frac{\mu_0}{\sqrt{\nu}} \frac{\partial \hat{\overline{\mathscr{T}}}_{12s}}{\partial \boldsymbol{s}}\right), \qquad u = 2\sqrt{t}. \tag{86}$$

This shows that the point $\boldsymbol{s}(u)$ is driven towards the minimum of the u-dependent potential given by the quantity in brackets. By symmetry the motion takes place in a polar plane, say the $(s_x s_z)$-plane. As u tends to infinity the first term in brackets tends to zero, so that $\boldsymbol{s}(u)$ tends to the minimum of $\hat{\overline{\mathscr{T}}}_{12s}$ at $(s_x, s_z) = (s_m, 0)$. This implies that the relative distance vector tends towards $\boldsymbol{R}_m(t) = \sqrt{4\nu t}(s_m, 0, 0)$, with distance increasing as $\sqrt{t}$.

6. Discussion

We have endeavoured to calculate the kinetic energy of the transient flow about a single sphere and about a pair of spheres moving in a viscous fluid after a suddenly applied impulse. At short times the kinetic energy follows from the theory of potential flow and is used conventionally to calculate effective mass and interaction energy. At long times the flow shows scaling behaviour. In this regime the kinetic energy decays with a $t^{-3/2}$ power law. We have also considered the transient flow after a constant applied force is applied starting from rest at time $t = 0$. For a pair of spheres the energy depends parametrically on the distance vector between the two centres. We have argued that this dependence gives rise to a hydrodynamic force acting between the two spheres. The distance-dependence of the force in the scaling regime is in

qualitative agreement with the experiments of Jayaweera *et al.* (1964) on settling spheres.

Time-dependent hydrodynamic interactions between two spheres have been measured experimentally for two trapped spheres (Atakhorrami *et al.* 2005), corresponding to the frequency-dependent response in the linear regime. The additional interaction discussed above is nonlinear and quadratic in the applied force. It follows from a reciprocal theorem (Kim & Karrila 1991) that in the linear regime the relative distance vector between a pair of identical settling spheres remains constant. The distance vector changes only owing to the nonlinear interaction.

Small inertial effects in steady flow in the presence of one or two walls have been studied by many authors, both experimentally and theoretically (Brenner 1966; Leal 1980; Feuillebois 2004). The calculations are based on a solution of the Navier–Stokes equations in regular or singular perturbation theory. Most of the calculations pertain to a single particle, not necessarily spherical. It has been suggested that the motion tends to a final steady state of minimum dissipation (Jeffery 1922), but experimentally states of maximum dissipation have been observed (Karnis, Goldsmith & Mason 1966). Inertial interactions between two disks confined by two lines were studied in lattice-Boltzmann simulations by Aidun & Ding (2003).

Elsewhere we have performed a calculation of the kinetic energy of the flow generated by two steadily settling distant particles between two walls, and suggested that the distance-dependence of the energy in the limit of widely separated walls gives rise to a repulsive interaction force (Felderhof 2005). The present calculation in the transient regime is far simpler, because it is not necessary to introduce walls and the calculation can be performed in infinite space. It would be worthwhile to compare the theory for the transient regime with experiment and computer simulation.

REFERENCES

Abramowitz, M. & Stegun, I. A. 1965 *Handbook of Mathematical Functions.* Dover.

Aidun, C. K. & Ding, E.-J. 2003 Dynamics of particle sedimentation in a vertical channel: Period-doubling bifurcation and chaotic state. *Phys. Fluids* **15**, 1612.

Albano, A. M., Bedeaux, D. & Mazur, P. 1975 On the motion of a sphere with arbitrary slip in a viscous incompressible fluid. *Physica* A **80**, 89.

Atakhorrami, M., Koenderink, G. H., Schmidt, C. F. & MacKintosh, F. C. 2005 Short-time inertial response of viscoelastic fluids: observation of vortex propagation. *Phys. Rev. Lett.* **95**, 208302.

Brenner, H. 1966 Hydrodynamic resistance of particles at small Reynolds number. *Adv. Chem. Engng* **6**, 287.

Cichocki, B. & Felderhof, B. U. 2000 Long-time tails in the solid-body motion of a sphere immersed in a suspension. *Phys. Rev.* E **62**, 5383.

Einstein, A. 1906 Zur Theorie der Brownschen Bewegung. *Ann. Phys. (Leipzig)* **19**, 371; reprinted in English translation in 1956 *Investigations on the Theory of the Brownian Movement* (ed. R. Fürth). Dover.

Felderhof, B. U. 1976 Force density induced on a sphere in linear hydrodynamics, II. Moving sphere, mixed boundary conditions. *Physica* A **84**, 557, erratum 1977 *Physica* A **88**, 617.

Felderhof, B. U. 1991 Motion of a sphere in a viscous incompressible fluid at low Reynolds number. *Physica* A **175**, 114.

Felderhof, B. U. 2005 Sedimentation of spheres at small Reynolds number. *J. Chem. Phys.* **122**, 214905.

Felderhof, B. U. 2007*a* Flow caused by a square force pulse applied to a sphere immersed in a viscous incompressible fluid. *Phys. Fluids* **19**, 093102.

Felderhof, B. U. 2007*b* Transient flow caused by a sudden impulse or twist applied to a sphere immersed in a viscous incompressible fluid. *Phys. Fluids* **19**, 073102.

Felderhof, B. U. 2007*c* Effect of fluid compressibility on the flow caused by a sudden impulse applied to a sphere immersed in a viscous fluid. *Phys. Fluids* **19**, 126101.

Felderhof, B. U. & Jones, R. B. 1986 Hydrodynamic scattering theory of flow about a sphere. *Physica* A **136**, 77.

Feuillebois, F. 2004 *Perturbation Problems at Low Reynolds Number*. Institute of Fundamental Technological Research.

Happel, J. & Brenner, H. 1973 *Low Reynolds Number Hydrodynamics*, p. 504. Noordhoff.

Hocking, L. M. 1964 The behaviour of clusters of spheres falling in a viscous fluid. *J. Fluid Mech.* **20**, 129.

Jayaweera, K. O. L. F., Mason, B. J. & Slack, G. W. 1964 The behaviour of clusters of spheres falling in a viscous fluid. *J. Fluid Mech.* **20**, 121.

Jeffery, G. B. 1922 The motion of ellipsoidal particles immersed in a viscous fluid. *Proc. R. Soc. Lond.* A **102**,161.

Karnis, A., Goldsmith, H. & Mason, S. G. 1966 The flow of suspensions through tubes. Part 5. Inertial effects. *Can. J. Chem. Engng* **44**, 181.

Kim, S. & Karrila, S. J. 1991 *Microhydrodynamics: Principles and Selected Applications*, p. 154. Butterworth-Heinemann.

Lamb, H. 1932 *Hydrodynamics*, p. 130. Dover.

Leal, L. G. 1980 Particle motion in a viscous fluid. *Annu. Rev. Fluid Mech.* **12**, 435.

Lighthill, J. 1986 *An Informal Introduction to Theoretical Fluid Mechanics*. Clarendon.

Onsager, L. 1931 Reciprocal relations in irreversible processes. II . *Phys. Rev.* **38**, 2265.

Oseen, C. W. 1927 *Hydrodynamik*, p. 47. Akademische Verlagsgesellschaft.